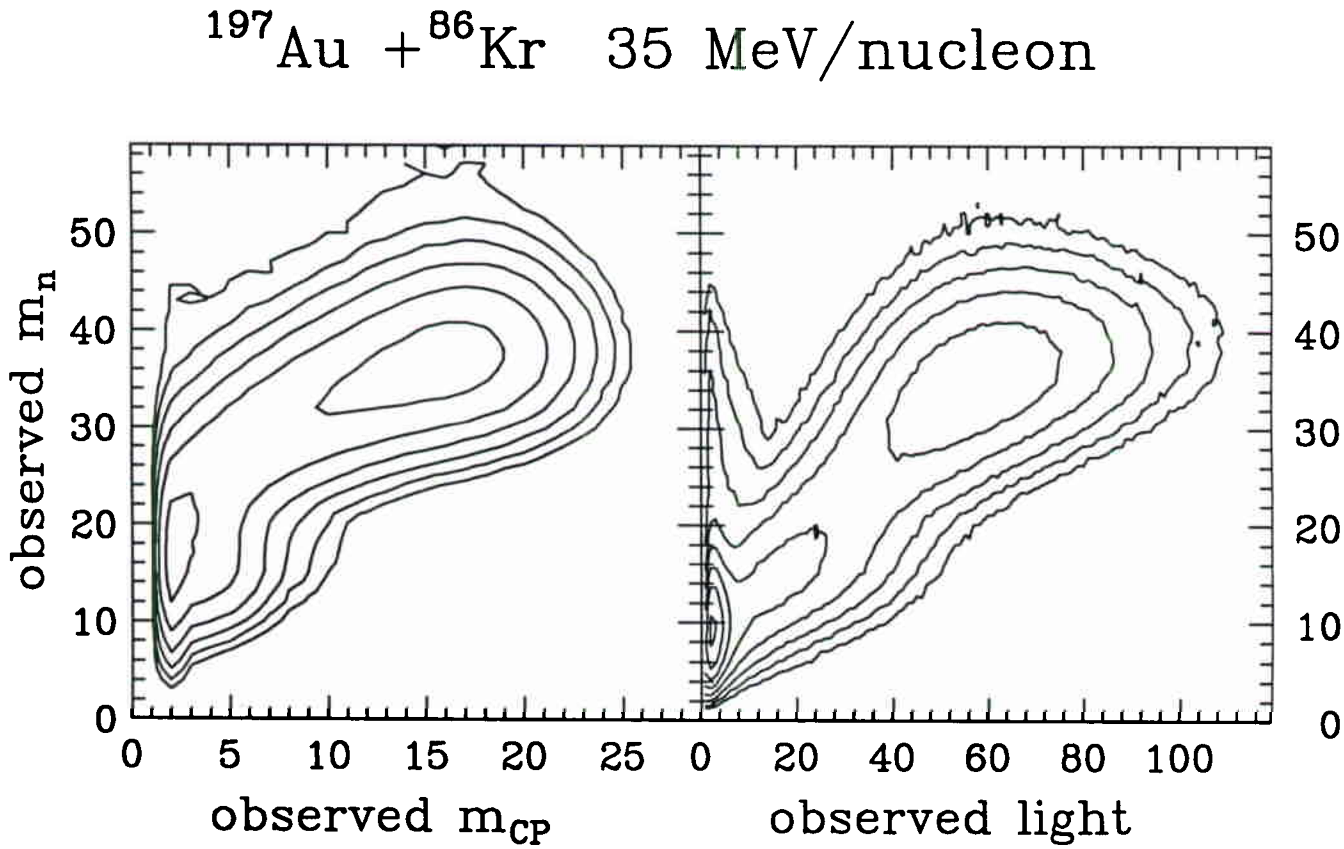

Fig.VIII.6: Contour diagrams of the correlations between multiplicity of neutrons (m_n) and charged-particle multiplicity (m_{cp}) (left panel) or the prompt light output (right panel). The contour lines are for constant number of counts increasing linearly in steps of 100.

the prompt light output (right panel). The contour lines are for constant number of counts increasing linearly in steps of 100. The m_n-m_{ncp} multiplicity correlation shown on the left has not been corrected for background ($m_b \approx 6$) yet, but is characteristic for a dissipative reaction involving a relatively heavy system and can be compared to that for the ^{209}Bi+^{136}Xe reaction displayed in Fig. II.1. In both figures, one observes the yield forming a vertical ridge at low charged-particle multiplicities, reaching up to $m_n \approx 20$, before the multiplicities m_n and m_{ncp} become correlated with each other. It is only for this latter part of the correlation, i.e., for moderate to high values of the dissipated energy, that both m_n and m_{ncp} become equivalent indicators of the degree of dissipation in a collision and its impact parameter. The panel on the right-hand side of Fig. VIII.6 displays the correlation between multiplicity and total kinetic energy of neutrons emitted in the ^{197}Au+^{86}Kr reaction, with the latter observable represented by the summed light output of the *SuperBall*. The correlation demonstrates that neutron multiplicity and light output are equivalent variables to characterize the degree of dissipation of a collision, for a range of multiplicities. For the highest musltiplicities, the correlation seems to become weaker, indicating a faster increase in the kinetic energy than in multiplicity of neutrons. These features are potentially very interesting have but to be explored in more detail.

Fig. VIII.7 and 8 display neutron multiplicity and prompt light output spectra from the *SuperBall*, taken with different trigger conditions, as defined by the coincident reaction products measured in a forward telescope. For example, Fig. VIII.7 shows the dependence of the neutron multiplicity on the degree of energy dissipation in a ^{197}Au+^{86}Kr collision, represented by quasi-elastic (upper right panel) and damped (lower left panel) events. The panel on the lower right of Fig. VIII.7 corresponds to a range of energy damping representing light charged particles or intermediate-mass fragments. The panel on the upper left represents the total ("ungated") multiplicity distribution, summed over all coincident events detected by the trigger telescope. The distinct peak at multiplicity $m_n \approx 6$ represents the random background. This peak is also dominant for quasi-elastic events, but is reduced to a shoulder on the multiplicity distribution measured in coinci-

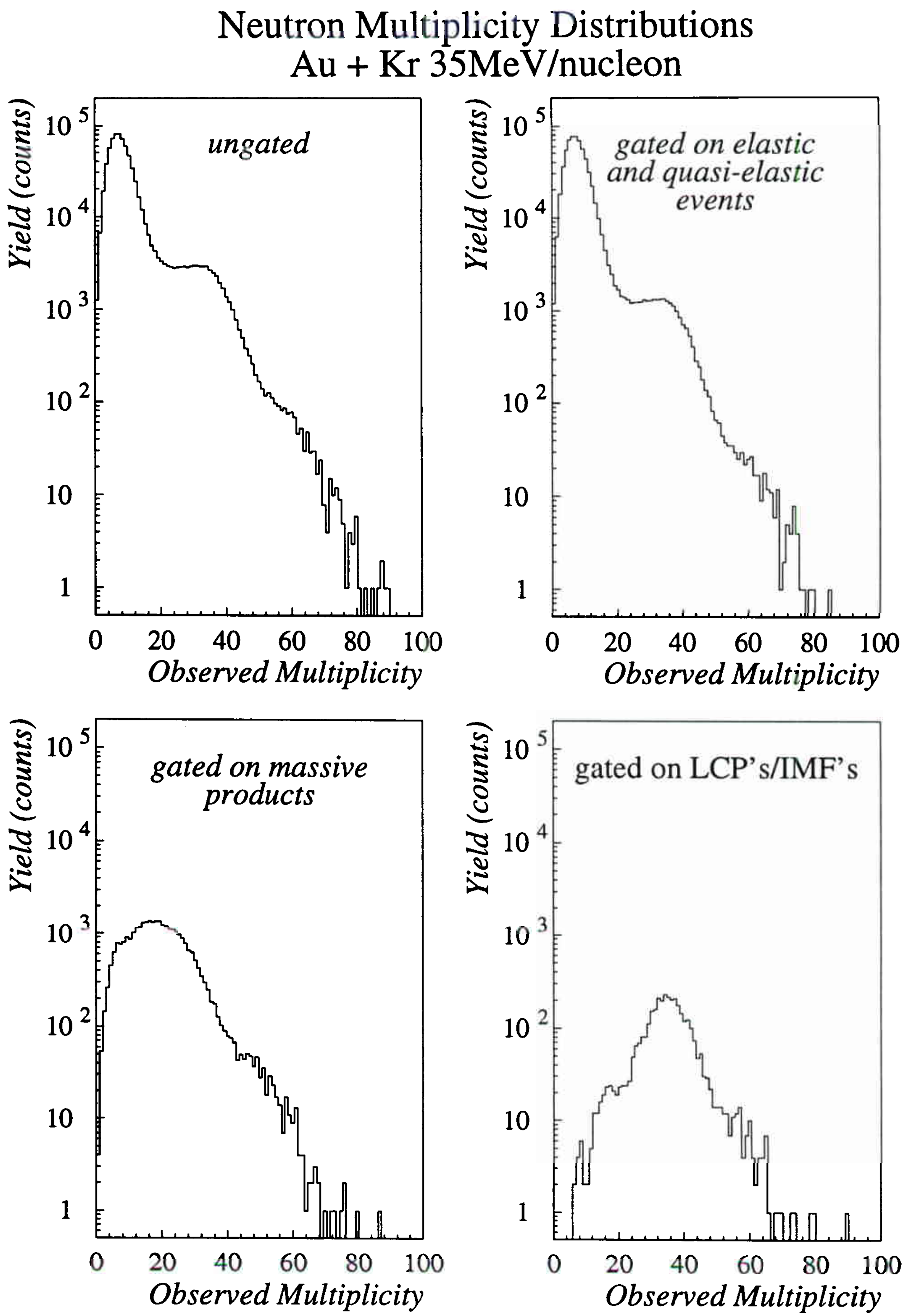

Fig. VIII.7: Neutron multiplicity distributions for the ^{197}Au+^{86}Kr reaction at E/A = 35 MeV, taken with different trigger fragments measured in a forward telescope.

dence with massive fragments, and has vanished for products associated with higher degrees of damping. To obtain the true neutron multiplicity distribution, the background has to be unfolded from the observed distribution.

In Fig. VIII.8, the light-output spectra of somewhat lower statistics are shown, for the same groups of events representing the corresponding panels in Fig. VIII.7. One observes that a noise component is peaked very sharply at low light output amplitudes and comprises a relatively smaller fraction of the spectrum than is the case for the multiplicity distributions. Otherwise, there is a dependence of the spectrum on the degree of energy damping which is quite similar to that observed with the multiplicity distributions, as expected from the correlations between these two observables discussed in the context of Figs. VIII.4 and 6.

The role of the *SuperBall* prompt-response light output can be examined further in Fig. VIII.9, where fragment-Z distributions from the ^{197}Au+^{86}Kr reaction are shown on logarithmic scale, from top to bottom gated with increasing light output amplitude. For this purpose, the light output spectrum (see Fig. VIII.5) was divided into roughly four equal bins. The spectrum at the top is the total spectrum, dominated by a quasi-elastic peak with $Z \approx 36$, the atomic number of the projectile, followed by a very broad, featureless distribution towards lower Z values. For $Z \lesssim 3$, an additional peak is seen in these distributions. One observes that, with increasing light output, the peak at high Z-values broadens and shifts toward lower atomic numbers. At the highest light output values, the product Z distribution does no longer provide evidence for a massive projectile-like fragment surviving the reaction and the subsequent decay processes. These distributions demonstrate a significant disassembly of the primary products into smaller clusters.

In Fig. VIII.10, raw experimental data are shown from the most recent experiment involving the *SuperBall*, the *MiniBall/Wall* array, as well as various other detectors. Here, the ^{112}Sn +^{112}Sn reaction was studied at E/A = 40 MeV. No corrections for background or efficiency have been applied yet to the data displayed in Fig. VIII.10. The upper left

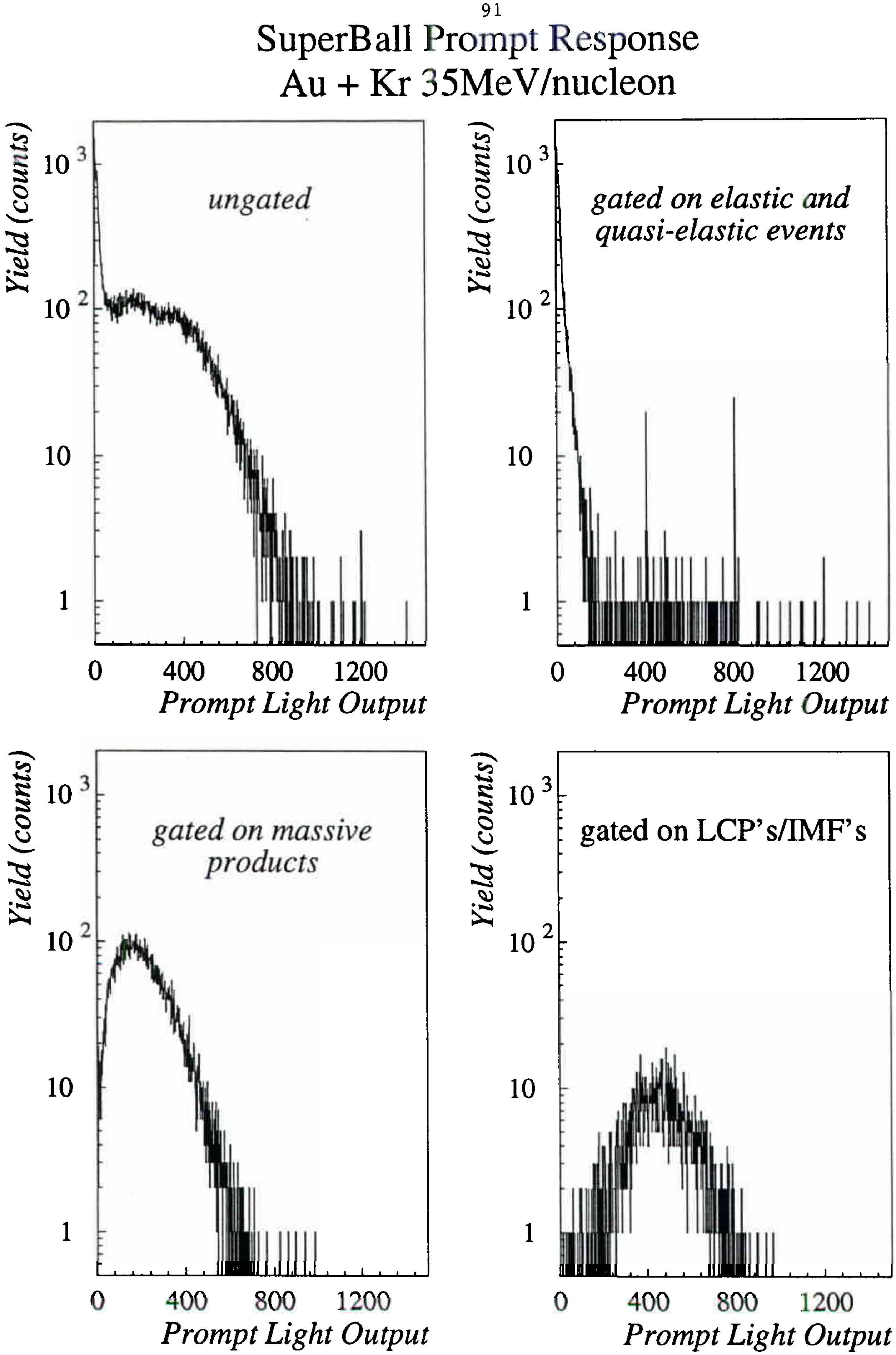

Fig. VIII.8: Light output spectra measured for the $^{197}Au+^{86}Kr$ reaction at E/A = 35 MeV, taken with different trigger fragments measured in a forward telescope.

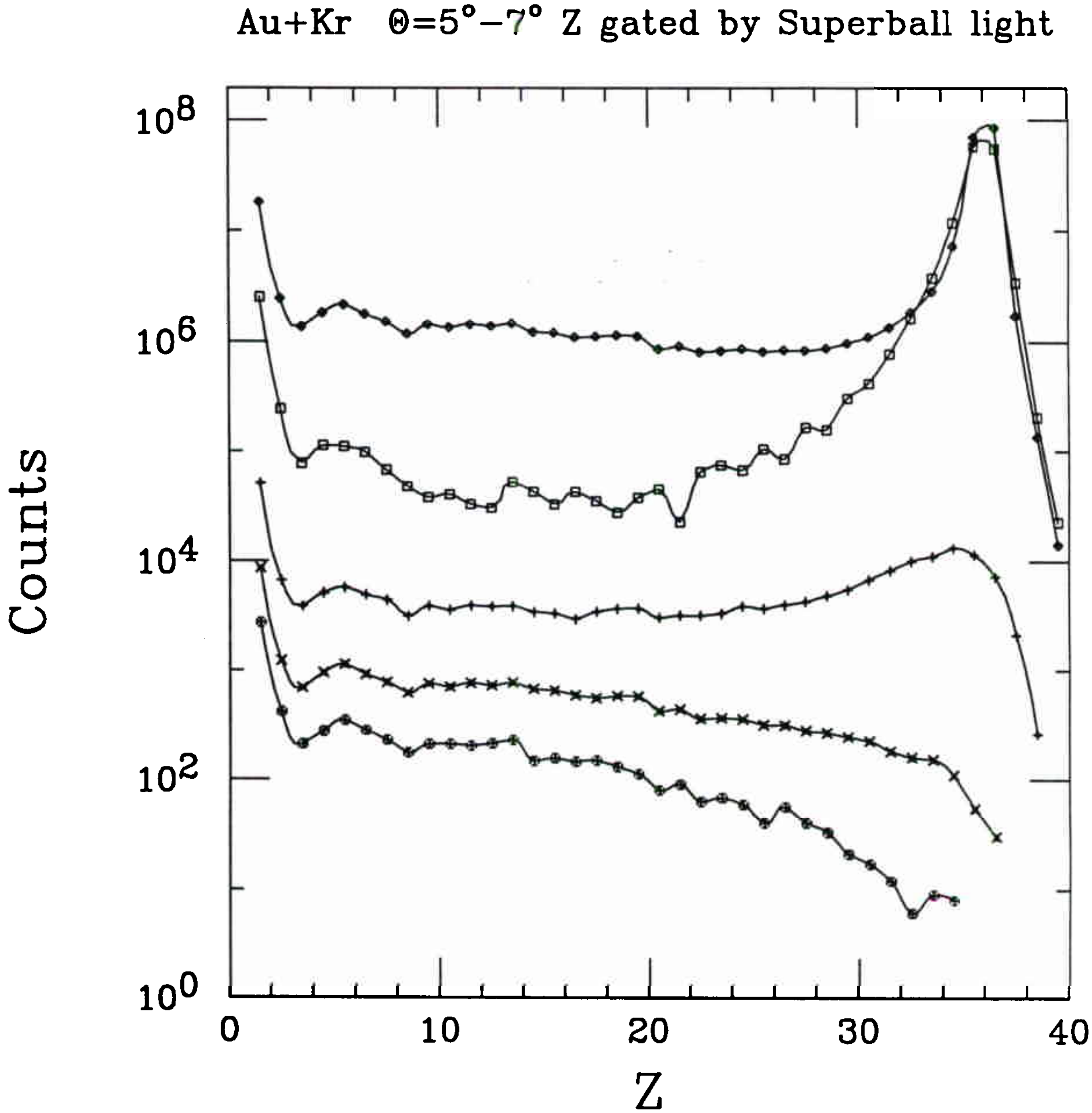

Fig. VIII.9: Fragment-Z distributions from the $^{197}Au+^{86}Kr$ reaction, from top to bottom gated with increasing light output amplitude, dividing the light output spectrum (see Fig. VIII.5) into roughly four equal bins. The spectrum at the top is the total spectrum.

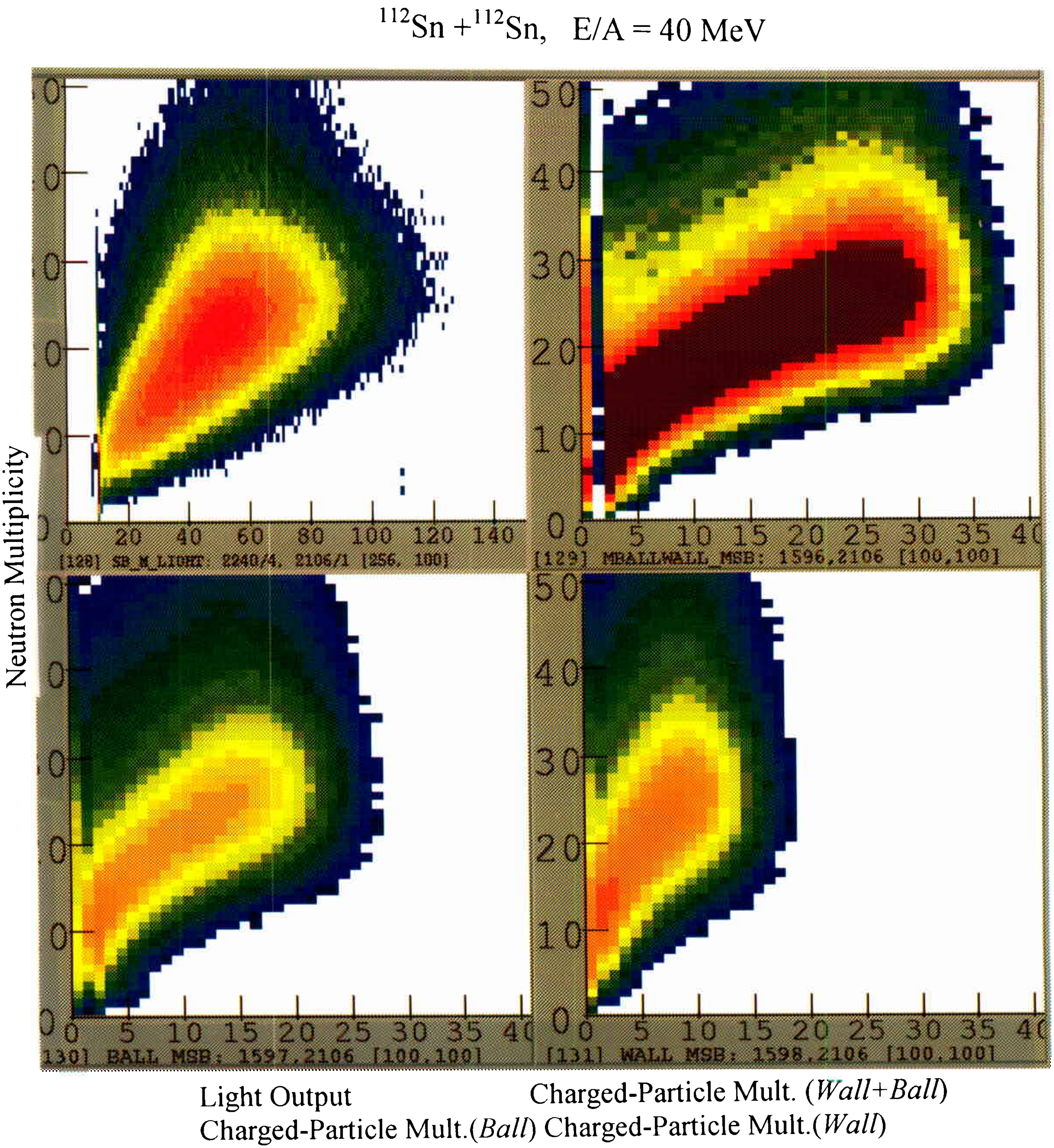

Fig. VIII.10: Raw experimental data from the $^{112}Sn + ^{112}Sn$ reaction at E/A = 40 MeV. No corrections for background or efficiency have been applied yet to the data. The upper left panel shows the correlation between neutron multiplicity m_n (ordinate) and prompt light output (abscissa) measured with the *SuperBall* in singles mode. The upper right panel depicts the correlation between m_n and charged-particle multiplicity m_{cp}. The panels on the lower left and right show the similar correlations, but for the *MiniBall (left)* and *MiniWall* (right) detector arrays separately.

panel shows the correlation between neutron multiplicity m_n (ordinate) and prompt light output (abscissa) measured with the *SuperBall* in singles mode. The upper right panel depicts the correlation between m_n and charged-particle multiplicity m_{cp}. These two ^{112}Sn +^{112}Sn correlations are similar to those for the ^{197}Au+^{86}Kr reaction exhibited in Fig.VIII.6. The panels on the lower left and right of Fig. VIII.10 show similar correlations, but for the *MiniBall (left)* and *MiniWall* (right) detector arrays separately.

As expected for a dissipative reaction mode and the relatively neutron poor *^{112}Sn* isotope, the m_n - m_{cp} correlation (Fig. VIII.10, upper right), if properly corrected for the background multiplicity of $m_n \approx 6$, shows a similar importance of neutrons and charged-particle emission from the massive primary projectile-like and target-like fragments. This behavior is different from that of the more neutron-rich systems ^{209}Bi+^{136}Xe and ^{197}Au+^{86}Kr, discussed earlier, where neutron emission clearly dominates. Nevertheless, one concludes that very neutron-poor, still hot secondary fragments can be produced in dissipative ^{112}Sn +^{112}Sn collisions. This is an observation of significance to studies exploring critical behavior for hot nuclei.

The lower two panels of Fig. VIII.10 have technical, in addition to physical, significance. They show the m_n-m_{cp} correlations for charged particles emitted in relatively backward (left) and forward (right) directions. For a symmetric system such as ^{112}Sn +^{112}Sn and equal intrinsic detector efficiencies and solid angles, these two correlations should be identical. One has, therefore, an important consistency check for the simulation calculations performed to deduce the pertinent corrections.

The upper left panel of Fig. VIII.10 depicts a prompt light output-m_n correlation slightly different from those measured for the more neutron-rich systems. Although there is clearly a correlation between light output an neutron multiplicity, the ^{112}Sn +^{112}Sn distribution suggests the existence of some degree of anticorrelation, for the highest multiplicities. Further study is needed to show to what extent these two observables can be used interchangeably. It is clear, however, that the combined measurement of both should give a more precise information than each of the individual observables. It is of experimental importance that a measurement of the prompt response is accomplished in a much shorter time (~ 0.1 μs) than counting the individual neutrons (~100 μs). Hence, the detector can sustain much higher count rates and measure smaller cross sections, when driven in such a "fast mode", where only the prompt response is recorded. The approximate conversion to neutron multiplicity can be achieved by a calibration measurement at low count rate, where multiplicity and light output can both be measured accurately.

IX. Summary and Outlook

The previous sections have outlined some of the motivation for constructing a large, high efficiency neutron calorimeter such as the *SuperBall* and have presented some of the more important details of its design and construction. The first in-beam tests have shown that the detector functions according to design goals. However, although it was found that the detector can be applied successfully in heavy-ion reaction studies at intermediate energies, these tests are not yet complete. There are some technical details which can, perhaps, be improved on. For example, moving the individual segments on their rails will have to be facilitated by some pulley mechanism or motorization. Checking the performance of the individual segments on-line and matching the photomultiplier gains could perhaps be improved. In the present realization, this information is acquired from a continuous measurement of a low-activity ^{252}Cf fission-neutron source.

Further investigations will show whether it is possible, as suggested by simulation calculations, to make a more efficient use of the prompt-response signal than in past applications of such detectors. This refers to a determination of the azimuthal angular distribution of neutrons from the asymmetry in response by the individual photomultipliers of a given tank. One would also like to be able to use the prompt-response signal to measure the total kinetic neutron energy on an absolute scale, requiring further in-beam calibration measurements. The correlation between multiplicity and total kinetic energy of the neutrons should also be investigated in more detail, since this is a potentially interesting variable that could be used to distinguish statistical evaporation from other processes. Some system dependence of this correlation has already been observed, as exemplified by the first reaction data obtained with the SuperBall presented in the previous section. It would also be interesting to see, whether or not the combination of multiplicity and energy would provide a more sensitive indication of the excitation of the emitters than either of the variables alone.

Furthermore, since the detector has an almost unit efficiency for detecting a neutron, even if it is not captured, the detector driven in the "fast mode" is a very efficient device for measuring reaction cross sections. This feature will become very useful in applications with secondary, low-intensity beams.

X. Acknowledgments

The work discussed in this report has been performed over the last three years by the University of Rochester Nuclear Chemistry Group, in particular by X. Zhao, S.P. Baldwin, D.K. Agnihotri, S.A. Masserant, and J. Tõke. Experiments with the *SuperBall* were conducted at MSU/NSCL in collaboration with groups from Washington University, Michigan State University, Oregon State University, and University of Uppsala.

There are a great many people who have made important contributions to the design, the construction, and the installation of the *SuperBall*. Certainly, building the detector would not have been possible without the technical competence and personal interest taken in the project by engineers such as Mr. Fonzi (formerly *DMI*) and Mr. Ottarson (*MSU/NSCL*). The construction of the major mechanical components at *Fab-Alloy* was led very efficiently by Ms. Levy. The outstanding quality of the work by her personnel is highly appreciated. Thanks are due to Mr. Mirski of *National Diagnostics* for his cooperation in developing a custom-made scintillator, and Mr. Davison of *Thorn EMI* for his part in furnishing efficient and economic electronic equipment for the detector. The workmanship of the personnel of the University of Rochester chemistry shops, Mr. Quinn and Mr. Carr, in the fabrication of scattering chamber and numerous other parts is also acknowledged.

The installation of the *SuperBall* at MSU/NSCL has required the commitment of considerable resources in funds and personnel by the laboratory, made by its directors Prof. Austin and Prof. Gelbke. Thanks are due to the NSCL technical staff who worked so effectively for the project. Dr. Sanderson, in particular, deserves sincere thanks for his efforts with the installation of the detector in the S-2 vault. Safety issues were handled very effectively by the various administrative offices involved at Michigan State University and the University of Rochester.

The project has enjoyed significant commitment and support by the University of Rochester, in particular by the Department of Chemistry, which is gratefully acknowledged here.

We also acknowledge partial support by the National Science Foundation through the use of its *National Superconducting Cyclotron Laboratory.*

This work was supported by the United States Department of Energy under grant agreements DE-FG05-91ER79048 and DE-FG02-88ER40414.

XI. References

Ayi87 S. Ayik, Phys. Rev. **C35**, 2086(1987)

Bar90 H.W. Barz et al., Phys. Let. **B244**, 161 (1990)

Bar92 H.W. Barz et al., Phys. Rev. **C46**, R42 (1992)

Ber88 G.F. Bertsch and S. Das Gupta, Phys. Rep. **160**, 189 (1988), and references cited therein.

Bon85 J.P. Bondorf et al., Nucl. Phys. **A443**, 321 (1985), ibid. **A444**, 460 (1985)

Bon87 A. Bonasera et al., Nucl. Phys. **A463**, 653 (1987)

Bro89 U. Brosa et al., Nucl. Phys. **A502**, 423c (1989)

Day86 R. Dayras et al., Nucl. Phys. **A460**, 299 (1986).

Div58 B.C. Diven et al., Phys. Rev. **109**, 144 (1958)

Div60 B.C. Diven et al., Phys. Rev. **120**, 556 (1960)

Fri83 W.A. Friedman, Phys. Rev. **C27**, 569 (1983); ibid. **C28**, 16 (1983)

Fri88 W.A. Friedman, Phys. Rev. Let. **60**, 2125 (1988)

Fri90 W.A. Friedman, Phys. Rev. **C42**, 667 (1990)

Gal90 J. Galin et al., Proc. Symp. Heavy-Ion Coll., Obernai, (World Scientific, 1990)

Gol74 A.S. Goldhaber, Phys. Lett. **B53**, 306 (1974)

Gra88 O. Granier et al., Nucl. Phys. **A481**, 109 (1988)

Gre86 C. Gregoire and B. Tamain, Ann. Phys. Fr. **11**, 323 (1986), and references cited therein.

Gro86 D.H.E. Gross et al., Phys. Rev. Lett. **56**, 1544 (1986)

Gro87 D.H.E. Gross et al., Nucl. Phys. **A461**, 641 (1987); ibid. **A461**, 668 (1987)

Gro93 D.H.E. Gross et al., Prog. Part. Nucl. Phys. **30**, 155 (1993), and references cited therein.

Jah83 U. Jahnke et al., Lecture Notes in Physics (Springer Verl. Berlin) **178**, 179 (1983)

Jia89 D.X. Jiang et al., Nucl. Phys. **A503**, 560 (1989)

Kim92 Y.D. Kim et al., Preprint MSUCL-850 (1992)

Lev87 S. Levit and P. Bonche, Nucl. Phys. **A462**, 109 (1987)

Lop89 J. A. Lopez and J. Randrup, Nucl. Phys. **A503**, 183 (1989)

Lop90 J. A. Lopez and J. Randrup, Nucl. Phys. **A512**, 345 (1990)

Lot93 B. Lott et al., Z. Phys. **A346**, 201 (1993)

Mor88 L.G. Moretto and G.J. Wozniak, Progr. Part. Nucl. Phys. **21**, 401 (1988).

Mor92 L.G. Moretto et al., Phys. Rev. Let. **69**, 1884 (1992)

Nic92 N.G. Nicolis et al., Comp. Phys. Comm., in press

Ogi92 C.A. Ogilvie et al., Phys. Rev Lett. **67**, 1214 (1992)

Pad91 D. Pade et al., Phys. Rev. C, **43**, 1288 (1991)

Pie93 L. Pienkowski et al., Nouvelles du GANIL 47, 37 (1993)

Poi74 J. Poitou et al., Nucl. Instr. Meth. **114**, 113 (1974)

Que93 B.M. Quednau, Ph.D. Thesis, Ruhr Univ. Bochum, 1993, unpublished

Sch80 W.U. Schröder, Nucl. Sci. Res. Conf. Ser. Vol.**2**, 19 (1980)

Sch84 W.U. Schröder and J.R. Huizenga, in *Treatise on Heavy-Ion Science*, (D.A. Bromley, Editor), Plenum Press (New York and London,1984), Vol.**2**, pp.113-726; and references cited therein

Sch92 W.U. Schröder, Nucl. Phys. **A539**, 493c (1992)

Sur87 E. Suraud, Nucl. Phys. **A462**, 109 (1987)

Sur 89 E. Suraud, Proc. Symp. Nucl. Dyn. Nucl. Disassembly, (J.B. Natowitz, editor) World Scientific, Singapore, 1989, p. 464.

Van73 R. Vandenbosch and J.R. Huizenga, *Nuclear Fission*, Academic Press (New York and London) 1973

Zha93 X. Zhao et al., Report DOE/ER/40414-6 (W. U. Schröder, editor), p.217 (1993)